

## Electron Delocalization Mediates the Metal-Dependent Capacity for CH/ $\pi$ Interactions of Acetylacetonato Chelates

Miloš K. Milčič,<sup>†</sup> Vesna B. Medaković,<sup>†</sup> Dušan N. Sredojević,<sup>†</sup> Nenad O. Juranić,<sup>‡</sup> and Snežana D. Zarić<sup>\*†</sup>

Department of Chemistry, University of Belgrade, Studentski trg 16, 11000 Belgrade, Serbia and Montenegro, and Department of Biochemistry and Molecular Biology, Mayo College of Medicine, Mayo Clinic and Foundation, Rochester, Minnesota 55905

Received November 8, 2005

CH/ $\pi$  interactions between the coordinated acetylacetonato ligand and phenyl rings were analyzed in the crystal structures from the Cambridge Structural Database and by quantum chemical calculations. The acetylacetonato ligand may engage in two types of interactions: it can be hydrogen atom donor or acceptor. The analysis of crystal structures and calculations show that interactions with the acetylacetonato ligand acting as hydrogen atom donor depend on the metal in an acetylacetonato chelate ring; the chelate rings with soft metals make stronger interactions. The same trend was not observed in the interactions where the acetylacetonato chelate ring acts as the hydrogen atom acceptor.

### Introduction

The noncovalent interactions of  $\pi$ -systems have been extensively studied in recent years. These interactions are important for many molecular systems from molecular biology to crystal engineering.<sup>1</sup> Noncovalent interactions involving metal atoms have gained particular attention with recognition that metal cations can bind to the phenyl ring by cation– $\pi$ -type interactions.<sup>2</sup> Cationic metal complexes are involved in similar metal–ligand aromatic cation– $\pi$  (MLAC $\pi$ ) interactions, where ligands coordinated to the metal interact with  $\pi$ -systems.<sup>3,4</sup> These can be considered also as a type of XH/ $\pi$  hydrogen bonds.<sup>4</sup>

Recently, it has been observed that planar chelate rings with delocalized  $\pi$ -bonds can be involved in noncovalent interactions in a manner similar to that in organic aromatic rings, indicating that these chelate rings could have aromatic character.<sup>5</sup> Both CH/ $\pi$  and stacking interactions with chelate rings were observed.<sup>6–10</sup> Analysis of the crystal structures of the metal complexes and quantum chemical calculations show that a chelate ring can be a hydrogen atom acceptor in CH/ $\pi$  interactions. Energy of the CH/ $\pi$  interactions with the chelate ring was evaluated by quantum chemical calculations to be about 1 kcal/mol. Geometries and energies of these

interactions are similar to the CH/ $\pi$  interactions with organic aromatic rings.<sup>7</sup> In our earlier study, we found that the chelate rings of the coordinated porphyrin can be also hydrogen acceptors in CH/ $\pi$  interactions.<sup>8,9</sup>

By coordination to metal atoms, the acetylacetonato ligand (acac) makes a planar chelate ring with the delocalized bonds. The acetylacetonato ligand has negative charge, but a partial positive charge is transferred from a metal cation to the ligand

- (1) (a) Desiraju, G. R.; Steiner, T. *The Weak Hydrogen Bonds in Structural Chemistry and Biology*; Oxford University Press: New York, 1999. (b) Steiner, T. *Angew. Chem., Int. Ed. Engl.* **2002**, *41*, 48–76. (c) Nishio, M. *Cryst. Eng. Comm.* **2004**, *6*, 130–158. (d) Nishio, M.; Hirota, M.; Umezawa, Y. *The CH/ $\pi$  Interaction. Evidence, Nature, and Consequences*; Wiley-VCH: New York, 1998. (e) Lovell, T.; Himo, F.; Han, W.; Noodleman, L. *Coord. Chem. Rev.* **2003**, *238*–239, 211–232. (f) Wang, T.; Quintanar, L.; Severance, S.; Solomon, E. I.; Kosman, D. J. *J. Biol. Inorg. Chem.* **2003**, *8*, 611–620. (g) Yanagisawa, S.; Sato, K.; Kikuchi, M.; Kohzuma, T.; Dennison, C. *Biochemistry* **2003**, *42*, 6853–6862. (h) Meyer, E. A.; Castellano, R. K.; Diederich, F. *Angew. Chem., Int. Ed. Engl.* **2003**, *42*, 1210–1250. (i) Niklas, N.; Zahl, A.; Alsfasser, R. *Dalton Trans.* **2003**, *5*, 778–786. (j) Laali, K. K.; Hupertz, S.; Temu, A. G.; Galembeck, S. E. *Org. Biomol. Chem.* **2005**, *3*, 2319–2326. (k) Novokmet, S.; Heine-mann, F. W.; Zahl, A.; Alsfasser, R. *Inorg. Chem.* **2005**, *44*, 4796–4805. (l) Li, Y.; Yang, C. M. *J. Am. Chem. Soc.* **2005**, *127*, 3527–3530. (m) Vondrasek, J.; Bendova, L.; Klusak, V.; Hobza, P. *J. Am. Chem. Soc.* **2005**, *127*, 2615–2619. (n) Pletneva, E. V.; Leaderach, A. T.; Fulton, D. B.; Kostić, N. M. *J. Am. Chem. Soc.* **2001**, *123*, 6232–6245. (o) Burhardt, T. P.; Juranić, N.; Macura, S.; Ajtai, K. *Biopolymers* **2002**, *63*, 261–272. (p) Yamauchi, O.; Odani, A.; Takani, M. *J. Chem. Soc., Dalton Trans.* **2002**, 3411–3421. (q) Schmitt, W.; Anson, C. E.; Hill, J. P.; Powell, A. K. *J. Am. Chem. Soc.* **2003**, *125*, 11142–11143. (r) Rodriguez, A.; Garcia-Vazquez, A. J.; Sousa-Pedrares, A.; Romero, J.; Sousa, A. J. *Organomet. Chem.* **2004**, *689*, 557–563.

\* To whom correspondence should be addressed. Fax: +381 11 184 330. E-mail: szaric@chem.bg.ac.yu.

<sup>†</sup> Department of Chemistry, University of Belgrade.

<sup>‡</sup> Department of Biochemistry and Molecular Biology, Mayo College of Medicine.

by coordination. If enough positive charge is transferred, the hydrogen atoms of acac ligand will get enough positive charge to interact with the phenyl ring (metal–ligand CH/ $\pi$  (MLCH/ $\pi$ ) interactions). Moreover, the coordinated acetylacetonato ligand can be involved in CH/ $\pi$  interactions as the hydrogen atom acceptor, similar to other planar chelate rings with the delocalized bonds.<sup>7</sup> Hence, the acac chelate can make CH/ $\pi$  interactions with the phenyl ring in two ways: as the hydrogen atom donor or acceptor.

The extent and nature of electron delocalization in the chelate ring can influence CH/ $\pi$  interactions. Conceivably, with the metal charge delocalization, some hydrogen atoms of the acac ligand can get a more positive charge and act as stronger H-donors. However, it is less clear if a better delocalization would make the  $\pi$ -system of the chelate ring a better hydrogen atom acceptor, considering the opposing influence of the metal charge transfer. Here, we report on CH/ $\pi$  interactions in acetylacetonato complexes that were obtained by searching and analyzing crystal structures in the Cambridge Structural Database (CSD) and by quantum chemical calculations. We observed and studied a metal-dependent capacity the CH/ $\pi$  interactions, which to our knowledge is the first example of such study.

### CSD search and Computational Methods

A Cambridge Structural Database (CSD, version 5.26, November 2004, 325 709 entries)<sup>11a</sup> search has been performed for metal complexes with coordinated acetylacetonato ligands using the program Quest3D.<sup>11b</sup> To find metal ligand CH/ $\pi$  (MLCH/ $\pi$ )

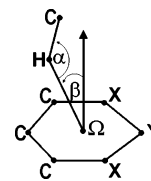


**Figure 1.** Geometrical parameters for the CH/ $\pi$  interaction with the phenyl ring (X, Y = C) or the acetylacetonato chelate ring (X = O, Y = M).

interactions with hydrogen atoms from the CH group of acetylacetonato ligand, we used geometrical criteria: distance between the H atom and the center of phenyl ring is shorter than 3.5 Å,  $\alpha$ , the angle between the C–H vector and center of phenyl ring, is in range of 110–180°,  $\beta$ , the angle between vector H atom center of the ring and vector normal to the ring, is smaller than 30° (Figure 1). The positions of hydrogen atoms were normalized.

To find MLCH/ $\pi$  interactions with a hydrogen atom from the CH<sub>3</sub> group, we used similar criteria. Because the phenyl ring could interact with any of three hydrogen atoms, we only used the criteria that the distance between the carbon atom and the center of the phenyl ring is smaller than 4.5 Å (Figure 1).

To find CH/ $\pi$  interactions with the phenyl ring as the hydrogen atom donor and the chelate ring as the hydrogen atom acceptor, we used the same criteria as for MLCH/ $\pi$  interactions with hydrogen atom of CH group: a distance shorter than 3.5 Å, the angle  $\alpha$  in the range of 110–180°, angle  $\beta$  smaller than 30°.

All ab initio and DFT energy calculations were carried out using the Gaussian 98 program.<sup>12</sup> Since crystal structures sometimes display unrelaxed intramolecular geometries yielding distorted wave functions and wrong energies, we optimized the geometries of the individual partners by DFT, specifically the Becke three-parameter exchange functional (B3)<sup>13</sup> and the Lee–Yang–Parr correlation functional (LYP).<sup>14</sup> For the initial estimate, the crystal coordinates were used. The LANL2DZ basis set was chosen for the metal atom (Pt, Pd, Ni, Rh, and Ir) and the 6-31G\*\* basis set was chosen for the carbon, oxygen, nitrogen, phosphorus, and hydrogen atoms. This hybrid DFT method was chosen because it gives good results for most complexes including first-row transition metals.<sup>15</sup> These optimized structures were then reassembled into geometries optimal for CH/ $\pi$  interactions. In the case of MLCH/ $\pi$  interactions, an interacting hydrogen atom from the transition-metal complex was

- (2) (a) Ma, J.; Dougherty, D. A. *Chem. Rev.* **1997**, *97*, 1303–1324. (b) Kim, D.; Hu, S.; Tarakeshwar, P.; Kim, K. S.; Lisy, J. M. *J. Phys. Chem. A* **2003**, *107*, 1228–1238. (c) Zhu, W.; Tan, X.; Shen, J.; Luo, X.; Cheng, F.; Mok, P. C.; Ji, R.; Chen, K.; Jiang, H. *J. Phys. Chem. A* **2003**, *107*, 2296–2303. (d) Amunugama, R.; Rodgers, M. T. *Int. J. Mass Spectrom.* **2003**, *227*, 339–360. (e) Vaden, T. D.; Lisy, J. M. *J. Chem. Phys.* **2004**, *120*, 721–730. (f) Hu, J.; Barbour, L. J.; Gokel, G. W. *Collect. Czech. Chem. Commun.* **2004**, *69*, 1050–1062. (g) Zhu, D.; Herbert, B. E.; Schlautman, M. A.; Carraway, E. R. *J. Environ. Qual.* **2004**, *33*, 276–284.
- (3) (a) Zarić, S. D. *Chem. Phys. Lett.* **1999**, *311*, 77–80. (b) Zarić, S. D.; Popović, D.; Knapp, E. W. *Chem.–Eur. J.* **2000**, *6*, 3935–3942. (c) Milčič, M. K.; Zarić, S. D. *Eur. J. Inorg. Chem.* **2001**, 2143–2150. (d) Šponer, J.; Šponer, J. E.; Leszczynski, J. *J. Biomol. Struct. Dyn.* **2000**, *17*, 1087–1096. (e) Zarić, S. D. *Eur. J. Inorg. Chem.* **2003**, 2197–2209. (f) Milčič, M. K.; Tomić, Z. D.; Zarić, S. D. *Inorg. Chim. Acta* **2004**, *357*, 4327–4329.
- (4) (a) Tsubaki, H.; Tohyama, S.; Koike, K.; Saitoh, H.; Ishitani, O. *Dalton Trans.* **2005**, *2*, 385–395. (b) Kumita, H.; Kato, T.; Jitsukawa, K.; Einaga, H.; Masuda, H. *Inorg. Chem.* **2001**, *40*, 3936–3942. (c) Suezawa, H.; Yoshida, T.; Umezawa, Y.; Tsuboyama, S.; Nishio, M. *Eur. J. Inorg. Chem.* **2002**, 3148–3155.
- (5) Masui, H. *Coord. Chem. Rev.* **2001**, *219–221*, 957–992.
- (6) Tomić, Z. D.; Novaković, S. B.; Zarić, S. D. *Eur. J. Inorg. Chem.* **2004**, 2215–2218.
- (7) Bogdanović, G. A.; Bire, A. S.; Zarić, S. D. *Eur. J. Inorg. Chem.* **2002**, 1599–1602.
- (8) Medaković, V. B.; Milčič, M. K.; Bogdanović, G. A.; Zarić, S. D. *J. Inorg. Biochem.* **2004**, *98*, 1867–1873.
- (9) Bogdanović, G. A.; Medaković, V.; Milčič, M. K.; Zarić, S. D. *Int. J. Mol. Sci.* **2004**, *5*, 174–185.
- (10) (a) Jiang, Y. F.; Xi, C. J.; Liu, Y. Z.; Niclós-Gutiérrez, J.; Choquesillo-Lazarte, D. *Eur. J. Inorg. Chem.* **2005**, 1585–1588. (b) Philip, V.; Suni, V.; Kurup, M. R. P.; Nethaji, M. *Polyhedron* **2004**, *23*, 1225–1233. (c) Castineiras, A.; Sicilia-Zafra, A. G.; Gonzáles-Pérez, J. M.; Choquesillo-Lazarte, D.; Niclós-Gutiérrez, J. *Inorg. Chem.* **2002**, *41*, 6956–6958. (d) Craven, E.; Zhang, C.; Janiak, C.; Rheinwald, G.; Lang, H. Z. *Anorg. Allg. Chem.* **2003**, *629*, 2282–2290. (e) Mukhopadhyay, U.; Choquesillo-Lazarte, D.; Niclós-Gutiérrez, J.; Bernal, I. *CrystrEngComm* **2004**, *6*, 627–632.
- (11) (a) Allen, F. H. *Acta Crystallogr., Sect. B* **2002**, *58*, 380–388. (b) Allen, F. H.; Davies, J. E.; Galloy, J. J.; Johnson, O.; Kennard, O.; Macrae, C. F.; Mitchell, E. M.; Mitchell, G. F.; Smith, J. M.; Watson, D. G. *J. Chem. Inf. Comput. Sci.* **1991**, *31*, 187–204.
- (12) Frisch, M. J.; Trucks, G. W.; Schlegel, H. B.; Scuseria, G. E.; Robb, M. A.; Cheeseman, J. R.; Zakrzewski, V. G.; Montgomery, J. A., Jr.; Stratmann, R. E.; Burant, J. C.; Dapprich, S.; Millam, J. M.; Daniels, A. D.; Kudin, K. N.; Strain, M. C.; Farkas, O.; Tomasi, J.; Barone, V.; Cossi, M.; Cammi, R.; Mennucci, B.; Pomelli, C.; Adamo, C.; Clifford, S.; Ochterski, J.; Petersson, G. A.; Ayala, P. Y.; Cui, Q.; Morokuma, K.; Malick, D. K.; Rabuck, A. D.; Raghavachari, K.; Foresman, J. B.; Cioslowski, J.; Ortiz, J. V.; Stefanov, B. B.; Liu, G.; Liashenko, A.; Piskorz, P.; Komaromi, I.; Gomperts, R.; Martin, R. L.; Fox, D. J.; Keith, T.; Al-Laham, M. A.; Peng, C. Y.; Nanayakkara, A.; Gonzalez, C.; Challacombe, M.; Gill, P. M. W.; Johnson, B. G.; Chen, W.; Wong, M. W.; Andres, J. L.; Head-Gordon, M.; Replogle, E. S.; Pople, J. A. *Gaussian 98*, revision A.6; Gaussian, Inc.: Pittsburgh, PA, 1998.
- (13) Becke, A. D. *J. Chem. Phys.* **1993**, *98*, 5648–5652.
- (14) Lee, C.; Yang, W.; Parr, R. G. *Phys. Rev. B* **1988**, *37*, 785–789.
- (15) (a) Zarić, S. D.; Hall, M. B. *J. Phys. Chem.* **1998**, *102*, 1963–1964. (b) Rovira, C.; Kunc, K.; Hutter, J.; Ballone, P.; Parrinello, M. *Int. J. Quantum Chem.* **1998**, *69*, 31–35. (c) Niu, S.; Thomson, L.; Hall, M. B. *J. Am. Chem. Soc.* **1999**, *121*, 4000–4007. (d) Niu, S.; Hall, M. B. *Chem. Rev.* **2000**, *100*, 353–406. (e) Galstyan, A. S.; Zarić, S. D.; Knapp, E. W. *J. Biol. Inorg. Chem.* **2005**, *10*, 343–354. (f) Medaković, V. B.; Zarić, S. D. *Inorg. Chim. Acta* **2003**, *349*, 1–5.

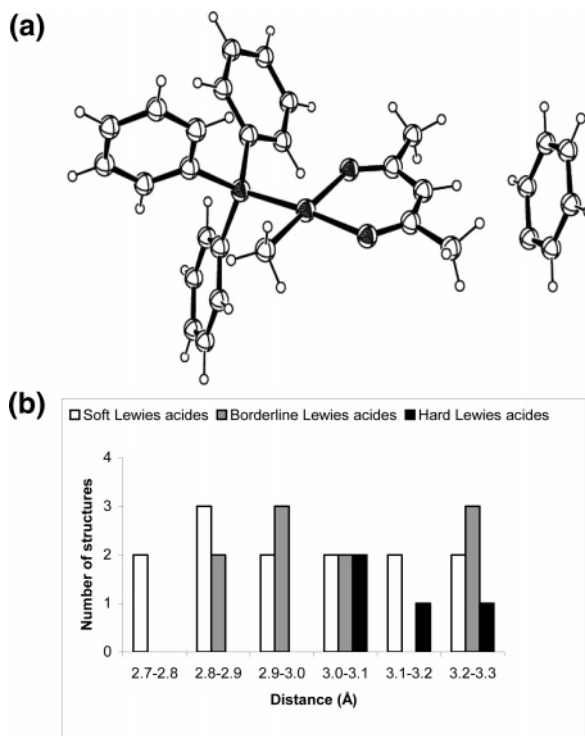


**Figure 2.** (a) Crystal structure of WANYUF<sup>18</sup> representing an example for MLCH/ $\pi$  interactions with the CH group of the acetylacetonato ligand. (b) Histogram showing the distribution of geometrical parameters for the MLCH/ $\pi$  interactions with the CH group of acetylacetonato ligand for complexes with soft, borderline, and hard Lewis acids.

put on the C<sub>6</sub> axis of a benzene molecule (i.e.,  $\alpha$  is constrained to 180° and  $\beta$  is constrained to 0°). In the case of interactions where a chelate ring acts as a hydrogen atom acceptor, the benzene molecule is put above center of chelate ring.

MP2 single point calculations were done on these B3LYP optimized structures with the same basis set. The interaction energy  $\Delta E$  is defined as the difference between the energy of the complex A–B and the energy of the isolated partners (i.e.,  $\Delta E = E(A-B) - E(A) - E(B)$ ). The standard counterpoise method was applied to correct interaction energies for the basis set superposition error (BSSE).<sup>16</sup>

The partial atomic charges of transition metal complexes were calculated using the natural bond orbital method developed by Weinhold<sup>17</sup> from the MP2 wave function.

## Results and Discussion

**CH/ $\pi$  Interactions in Crystal Structures. MLCH/ $\pi$  Interactions with the Phenyl Ring.** By searching CSD, we found a large number of structures where an acetylacetonato ligand (CH and CH<sub>3</sub> groups) is involved in interactions with a phenyl ring as a hydrogen atom donor. We found 32 interactions with the CH group and 584 interactions with the CH<sub>3</sub> groups. The much larger number of interactions with the CH<sub>3</sub> groups is caused by the larger number of hydrogen atoms in two CH<sub>3</sub> groups and by steric reasons. Examples of structures exhibiting interactions with CH and CH<sub>3</sub> groups are given in Figures 2a and 3a.

(16) Boys, S. B.; Bernardi, F. *Mol. Phys.* **1970**, *19*, 553–577.

(17) Reed, A. E.; Curtiss, L. A.; Weinhold, F. *Chem. Rev.* **1988**, *88*, 899–926.

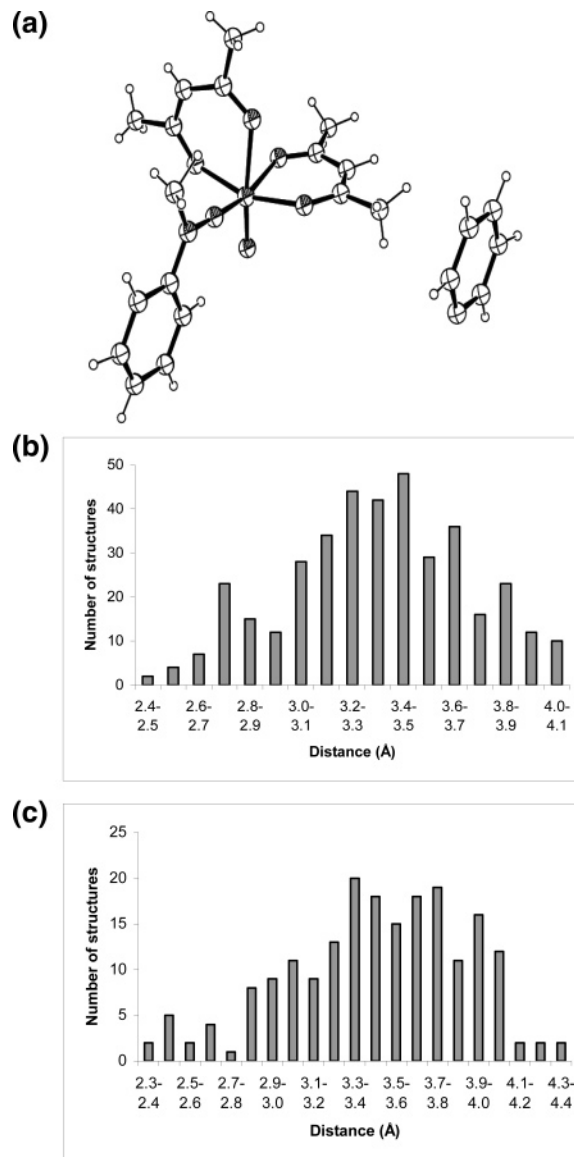


**Figure 3.** (a) Crystal structure of HAFRAH representing an example of MLCH/ $\pi$  interactions with the CH<sub>3</sub> group of the acetylacetonato ligand. Histograms showing the distributions of the H– $\Omega$  distances for (b) intermolecular and (c) intramolecular CH<sub>3</sub>–phenyl interactions.

**MLCH/ $\pi$  Interactions of CH Group with Phenyl Ring.** All found MLCH/ $\pi$  interactions with the CH group are intermolecular because of extended geometry of the acac chelate ring. An example for these interactions is given in Figure 2a. In Table 1 there are data for two distances, between center of the phenyl ring ( $\Omega$ ) and hydrogen (H $\cdots\Omega$ ) and C atom (C $\cdots\Omega$ ), and two angles,  $\alpha$  and  $\beta$  (Figure 1). The data show that the H– $\Omega$  distance is never shorter than 2.7 Å. The reason for this are steric constraints; a phenyl group cannot be closer to the CH group because of clashing with two CH<sub>3</sub> groups.

The strength of the CH/ $\pi$  interactions depends on the partial positive charge on hydrogen atom.<sup>1c,3e</sup> The acetylacetonato ligand is negatively charged, and it gets some positive charge by coordinating to a metal cation. Hence, the partial positive charge on hydrogen atom of the CH group depends on the delocalization in the chelate ring, while delocalization depends on bonding between the ligand and the metal. To

**Table 1.** Some Data<sup>a</sup> for the MLCH/ $\pi$  Interactions with the CH Group of the Acetylacetonato Ligand<sup>b</sup>

refcode	metal	complex charge	H... $\Omega$	C... $\Omega$	$\alpha$	$\beta$
soft Lewis acids						
TIFNIF	Os(II)	0	3.11	3.89	129.7	29.4
ACTBPD	Pd(II)	0	2.95	4.00	163.5	22.5
ACXMPD	Pd(II)	0	2.82	3.89	169.1	5.1
DOPYUC	Pd(II)	0	3.05	3.96	142.3	16.6
DOPYUC	Pd(II)	0	2.87	3.72	135.7	10.7
WANYUF	Pt(II)	0	2.80	3.86	160.7	2.7
DORVAH	Rh(I)	0	2.83	3.82	152.7	4.9
HOWRAM	Rh(I)	0	3.10	4.14	159.8	6.9
HUBTAZ	Rh(I)	0	3.09	4.08	151.6	10.7
HUBTAZ	Rh(I)	0	3.22	4.22	153.4	23.0
HUBTIH	Rh(I)	0	2.96	3.94	151.1	21.0
TOTVON	Rh(I)	0	2.73	3.72	151.7	19.1
YETJIQ	Rh(I)	0	3.20	3.86	120.3	27.7
borderline Lewis acids						
DAWQAT	Ru(III)	0	3.00	3.97	149.2	8.4
JUZLEV	Ru(II)	0	3.24	4.20	148.9	12.2
MEWXAN	Ir(III)	0	2.84	3.73	138.6	6.1
COWREL	Ru(II)	0	2.91	3.94	158.7	16.3
MANSOJ	Ru(II)	0	3.02	4.08	168.8	2.3
NIFNAR	Ru(II)	0	2.86	3.88	156.0	7.2
PIBTEZ	Ru(II)	+1	2.88	3.99	161.6	11.5
PUQTOK	Ru(II)	0	3.09	4.08	151.9	25.6
XIFYAM	Fe(II)	+1	3.45	4.43	150.2	27.7
YIPSOQ	Rh(III)	0	2.94	3.83	140.5	11.4
XIBSOQ	Ni(II)	0	3.24	4.25	156.0	29.6
PEMLUO	Cu(II)	0	3.21	3.86	119.3	25.6
hard Lewis acids						
PUFROX	Zr(IV)	0	3.03	3.85	119.3	25.6
HOXTIX	Ti(IV)	0	3.17	4.18	155.8	27.8
NICLUG	Ti(IV)	0	3.21	4.27	164.6	19.4
LOPGIG	Zr(IV)	0	3.00	4.09	178.6	12.3
KIQMOM	Cr(III)	+1	3.23	4.26	159.2	28.1
SAPJUO	Mn(III)	+1	3.29	4.35	166.5	27.2
PANTIH	Co(III)	+1	3.47	4.38	142.5	27.0

<sup>a</sup> Definitions of the geometrical parameters are given in Figure 1.

<sup>b</sup> References for crystal structures are given in the Supporting Information.

determine if the type of metal has influence on the H– $\Omega$  distances, the complexes in Table 1 were separated into three groups. In the first group, there are complexes with metals that are soft acids; the complexes with borderline acids are in the second group, and the third group contains the complexes with hard acids. The histogram in Figure 2b shows the H– $\Omega$  distances for different types of metals as acids for neutral complexes, since charge also can influence the H– $\Omega$  distances. The data show that complexes with soft acids have a tendency to make shorter H– $\Omega$  distances, while complexes with hard acids have a tendency to make longer H– $\Omega$  distances. All distances in complexes with hard acids are above 3.0 Å.

Metals that are soft acids can make covalent bonds with the acetylacetonato ligand. It enables the delocalization of the negative charge of ligand, increases the partial positive charge in the ligand, and makes stronger MLCH/ $\pi$  interactions with shorter H– $\Omega$  distances. In complexes with hard acids there is less covalent character of the metal–ligand bonds and less positive charge in the ligand, and the H– $\Omega$  distances are longer. Hence, complexes with better delocalization in chelate rings can make the MLCH/ $\pi$  interactions with phenyl rings stronger. The quantum chemical calculations supported this conclusion, as shown later.

Most of the complexes in Table 1 are neutral; there are just five complexes with a positive charge. In most cases, the interaction occurs between two equivalent molecules; the acac ligand from one molecule interacts with the phenyl group from another molecule, and in case of neutral complexes, there is no repulsion between molecules.

In positively charged acac complexes, there is a larger partial positive charge in the acac ligand that favors MLCH/ $\pi$  interactions with phenyl rings. In structure PIBTEZ,<sup>19</sup> the H– $\Omega$  distance is among shortest distances in the group (complexes with borderline acids): it is 2.88 Å (Table 1). In this structure only, a positively charged complex interacts with a neutral toluene molecule, and a larger positive charge on the ligand favors interaction with neutral phenyl ring. This is in agreement with previous results that show stronger interaction of positively charged complexes with benzene.<sup>3e</sup>

However, the positive charge has a repulsive effect in structures where two equivalent positively charged complexes interact. For that reason there are just a few structures with positively charged complexes in Table 1, and in these structures, the H– $\Omega$  distances are among the longest.

In the KIQMOM<sup>22</sup> and SAPJUO<sup>23</sup> structures, the phenyl ring is part of a tetraphenylborate anion. Previously it was shown that the strong MLCH/ $\pi$  interactions with short distances exist in structures where a tetraphenylborate anion interacts with cationic complexes.<sup>3f</sup> However in the present structures, the H– $\Omega$  distances are quite long, around 3.2 Å. The reason is the bulkiness of tetraphenylborate which prevents a close approach by the phenyl ring.

**MLCH/ $\pi$  Interactions of the CH<sub>3</sub> Groups with the Phenyl Ring.** MLCH/ $\pi$  interactions of CH<sub>3</sub>-group hydrogens are summarized in Figure 3b and c. The H– $\Omega$  distance histograms show a number of interactions for the hydrogen atom that is the closest to the center of phenyl ring. Different from the interactions with CH group, the intramolecular interactions are also possible, and we found a large number of both intramolecular and intermolecular interactions. There is no significant difference in the distribution of the distances for intermolecular and intramolecular interactions (Figure 3 b and c). Some H– $\Omega$  distances are quite short (for intermolecular, 2.4 Å and for intramolecular, even 2.3 Å) in comparison with the distances seen for the MLCH/ $\pi$  interactions of the CH group, which we attribute to the steric accessibility of the CH<sub>3</sub> group. However, the number of structures with short distances is not large.

To determine if metal-ion hardness has an influence on the H– $\Omega$  distances, as seen in the MLCH/ $\pi$  interactions of

- (18) Cavell, K. J.; Hong, J.; Skelton, B. W.; White, A. H. *J. Chem. Soc., Dalton Trans.* **1993**, 13, 1973–1978.
- (19) Schneider, R.; Weyhermuller, T.; Wieghardt, K.; Nuber, B. *Inorg. Chem.* **1993**, 32, 4925–4934.
- (20) Britovsek, G. J. P.; Gibson, V. C.; Spitzmesser, S. K.; Tellmann, K. P.; White, A. J. P.; Williams, D. J. *J. Chem. Soc., Dalton Trans.* **2002**, 6, 1159–1171.
- (21) Cardwell, T. J.; Edwards, A. J.; Hartshorn, R. M.; Holmes, R. J.; McFadyen, W. D. *Aust. J. Chem.* **1997**, 50, 1009–1016.
- (22) Muller, J.; Kikuchi, A.; Bill, E.; Weyhermuller, T.; Hildebrandt, P.; Ould-Moussa, L.; Wieghardt, K. *Inorg. Chim. Acta*, **2000**, 297, 265–277.
- (23) Wieghardt, K.; Pohl, K.; Bossek, U. *Z. Naturforsch. B* **1988**, 43, 1184–1194.

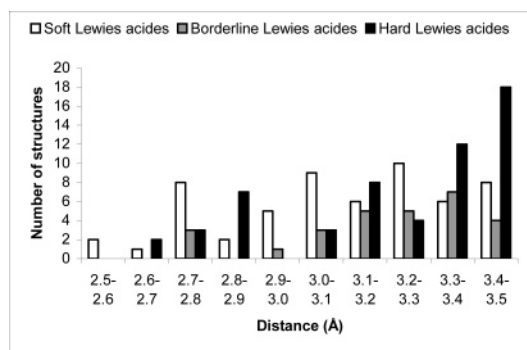


**Figure 4.** Histogram showing the distributions of the H- $\Omega$  distances for intermolecular CH<sub>3</sub>-phenyl interactions for neutral complexes with soft, borderline, and hard Lewis acids.

the CH group, we made the corresponding histograms for the neutral complexes (Figure 4). As before, there is tendency of the complexes with hard acids to make a weaker interaction (longer H- $\Omega$  distances).

**CH/ $\pi$  Interactions with the Chelate Ring as the Hydrogen Atom Acceptor.** In this type of interaction, the phenyl group is the hydrogen atom donor, while the delocalized  $\pi$ -system of the acac chelate ring is the hydrogen atom acceptor. An example of a structure with this interaction is shown in Figure 5a. We found 41 intermolecular interactions in 36 crystal structures in CSD and 30 intramolecular interactions in 22 crystal structures (Table 2 and Table 3). The shortest H- $\Omega$  distances are close to 2.4 Å, similar to those of the MLCH/ $\pi$  interactions with CH<sub>3</sub> group.

This is a different type of interaction, and we cannot expect that delocalization in the chelate ring will have the same influence as it does in the MLCH/ $\pi$  interactions; however, for comparison, the complexes in Table 2 were also separated in three groups: complexes with metals that are soft, borderline, and hard acids.

The bulkiness of the two interacting groups (two rings) makes steric effects very important; therefore, coordination geometry inherent to the type of the metal could have a dominant influence on these interactions. In the square-planar complexes, phenyl rings have an easier approach to the chelate rings, and the interacting distances can be shorter than in the case of octahedral complexes. Therefore, Figure 5b has separate histograms for square-planar and octahedral complexes. Soft and borderline metals make square-planar complexes, while borderline and hard metals make octahedral complexes. As anticipated, the H- $\Omega$  distances are shorter in the square-planar structures than in the octahedral complexes. The H- $\Omega$  distances for square-planar complexes with borderline metals are below 2.7 Å (with one exception), while they are over 3.0 Å in octahedral complexes. Data in the histogram for square-planar complexes indicate that there is some tendency of complexes with borderline metals to make stronger interactions than complexes with soft metals (Figure 5b). The complex with an exceptionally long distance has a lot of steric constraints. Hence, it seems that better delocalization of the negative charge in complexes with soft metals does not favor the interaction.

In octahedral complexes a chelate ring is less accessible for the interaction, and steric constraints have more influence

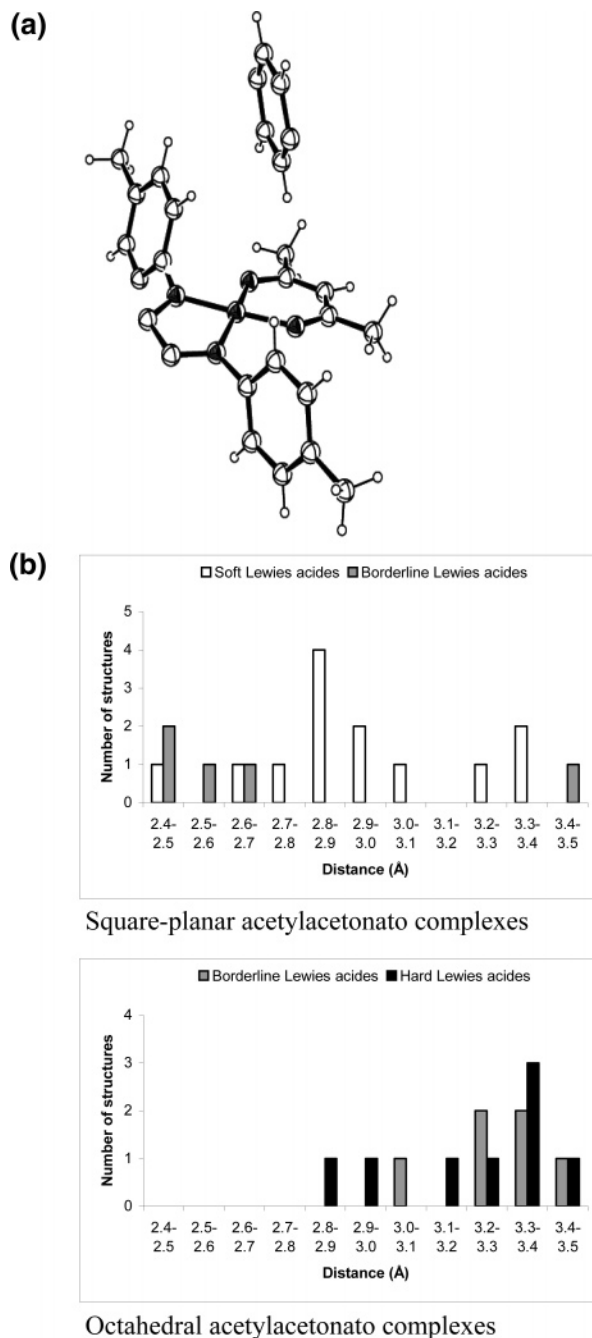


**Figure 5.** (a) Crystal structure of XIBRUV<sup>24</sup> representing an example of CH/ $\pi$  interactions with the chelate ring acting as the hydrogen atom acceptor. (b) Histograms showing the distributions of the H- $\Omega$  distances for the intermolecular CH-chelate interactions in neutral square-planar and octahedral complexes.

on the interactions; hence, one cannot expect to see the influence of the type of the metal in the complex. (Figure 5b).

Most of the complexes in Table 2 are neutral, and the interaction occurs between two equivalent molecules of a complex as was case with the complexes in Table 1. The reason is the same: in neutral molecules partial charges on both the phenyl and chelate rings are just suitable for the interaction.

There are only two examples of interactions of positively charged complexes and three for negatively charged complexes (Table 2). Significantly, the interaction also includes

**Table 2.** Some Data<sup>a</sup> for Intermolecular CH/ $\pi$  Interactions with the Chelate Ring as the Hydrogen Atom Acceptor<sup>b</sup>

refcode	metal	coordination geometry	complex charge	H... $\Omega$	$\alpha$	$\beta$
soft Lewis acids						
FIFPIT	Rh(I)	square-planar	0	2.73	141.6	17.3
TOTVON	Rh(I)	square-planar	0	3.09	151.5	23.7
ZOYRIO	Rh(I)	square-planar	0	2.93	148.2	28.4
DORVAH	Rh(I)	square-planar	0	2.80	123.8	11.1
HOWRAM	Rh(I)	square-planar	0	2.91	139.8	8.2
HUBTAZ	Rh(I)	square-planar	0	2.69	150.4	15.3
PUTZIN	Rh(I)	square-planar	0	2.49	153.1	6.6
PUTZIN	Rh(I)	square-planar	0	2.87	139.0	2.9
UDOZOC	Pd(II)	square-planar	0	2.84	167.9	25.6
UDOZOC	Pd(II)	square-planar	0	3.40	112.7	16.7
UDOZUI	Pd(II)	square-planar	0	2.86	166.4	25.3
WANYOZ	Pt(II)	square-planar	0	3.39	110.3	27.2
WANYUF	Pd(II)	square-planar	0	3.27	130.2	15.6
ZULMEY	Pd(II)	square-planar	+1	2.80	145.7	5.4
ZUZHOR	Pd(II)	square-planar	+1	2.66	133.2	11.9
borderline Lewis acids						
XUZBEZ	Mo(II)	octahedral	0	3.27	161.9	26.7
YIPNAM	Ir(III)	square-pyramidal	0	3.37	114.3	15.2
SOLJAE	Ru(III)	octahedral	-1	2.71	149.1	5.8
SOLJAE	Ru(III)	octahedral	-1	3.02	119.6	15.3
BAXZOP	Ru(II)	octahedral	0	3.33	140.9	18.8
PUKTOK	Ru(II)	octahedral	0	3.29	135.0	20.7
PUKTOK	Ru(II)	octahedral	0	3.05	143.2	20.8
MANSOJ	Ru(II)	octahedral	0	3.44	115.4	12.4
FOXHEF10	Fe(II)	tetrahedral	0	2.64	149.7	8.8
ACEYNI	Ni(II)	square-planar	0	3.41	136.7	17.9
NAKBWU	Ni(II)	octahedral	0	3.40	143.0	21.4
XIBRUV	Ni(II)	square-planar	0	2.63	167.0	8.6
XIBRUV	Ni(II)	square-planar	0	2.45	142.4	12.1
XIBRUV	Ni(II)	square-planar	0	2.57	158.9	8.9
XIBROP	Ni(II)	square-planar	0	2.46	156.6	3.6
PEMLUO	Cu(II)	square-pyramidal	0	3.11	174.7	28.8
hard Lewis acids						
HOXTAP	Ti(IV)	octahedral	0	3.37	119.1	10.5
NICLOA	Ti(IV)	octahedral	0	3.27	148.5	28.9
XISHUC	Ti(IV)	octahedral	0	2.96	138.4	15.2
PUFROX	Zr(IV)	cap. trigonal prismatic	0	3.13	116.8	14.0
PUFROX	Zr(IV)	cap. trigonal prismatic	0	2.81	145.7	5.8
TUKHEM	Mo(VI)	octahedral	0	3.32	130.2	9.3
TUKHAI	Mo(VI)	octahedral	0	2.96	152.0	12.9
TAKYEJ	Mn(III)	octahedral	0	3.37	140.4	4.6
XATZEP	Mn(III)	octahedral	0	2.85	144.4	24.2
ZAVCUU	Mn(III)	octahedral	0	3.12	146.8	16.0
COSNAC10	Co(III)	octahedral	0	3.45	139.8	20.1
SUKQUK	Co(III)	octahedral	-1	2.90	150.4	11.4

<sup>a</sup> Definitions of the geometrical parameters are given in Figure 1.  
<sup>b</sup> References for crystal structures are given in Supporting Information.

complexes with negative charge, while in case of MLCH/ $\pi$  they were absent. The negative charge of the complex increases electron density in the chelate ring and increases its proton accepting ability, and the interactions are quite strong. Moreover, short distances are also consequence of the attraction of positive and negative ions; in all three cases the phenyl ring is part of cation (SOLJAE,<sup>25</sup> SUKQUK<sup>26</sup>).

In the two structures with positively charged complexes, phenyl rings are part of the complex; hence, there is interaction between two equivalent molecules. In contrast to the interactions in Table 1, the H- $\Omega$  distances are not longer; in fact, they are quite short, 2.80 and 2.66 Å. It seems that the positive charge in the complex does not significantly affect the capability of the  $\pi$ -system of the chelate ring to participate in the interactions because the positive charge is

**Table 3.** Some Data<sup>a</sup> for Intramolecular CH/ $\pi$  Interactions with the Chelate Ring as the Hydrogen Atom Acceptor<sup>b</sup>

refcode	metal	complex charge	H... $\Omega$	$\alpha$	$\beta$
soft Lewis acids					
ADOBIE	Rh(I)	0	2.63	118.3	8.3
MULCUR	Rh(I)	0	2.35	126.0	12.3
QAJPEW	Rh(I)	0	2.63	110.1	5.4
DOHSOI	Rh(I)	0	3.18	138.3	28.7
DOHSOI	Rh(I)	0	3.13	139.8	29.0
MULCEB	Rh(I)	0	2.90	139.1	23.9
MULCEB	Rh(I)	0	3.05	139.4	28.4
MULCIF	Rh(I)	0	3.29	129.9	24.4
MULCOL	Rh(I)	0	2.69	139.5	23.1
borderline Lewis acids					
TUXVOX	Re(II)	0	2.73	145.4	27.7
TULDOT	Co(II)	0	2.62	110.7	17.6
NUSWAZ	Ni(II)	0	2.89	131.8	12.4
NUSWAZ	Ni(II)	0	2.56	125.1	11.1
YUZTAO	Ni(II)	0	2.68	126.7	11.4
YUZTAO	Ni(II)	0	2.56	128.3	9.0
YUZTAO01	Ni(II)	0	2.97	124.6	14.6
YUZTAO01	Ni(II)	0	2.68	126.7	11.4
YUZTAO01	Ni(II)	0	2.51	124.0	12.3
YUZTAO01	Ni(II)	0	2.56	128.3	9.0
PEMLUO	Cu(II)	0	2.47	134.6	8.7
PEMLUO	Cu(II)	0	2.61	123.0	9.4
TULDIN	Zn(II)	0	2.54	115.2	16.7
hard Lewis acids					
IGIKUE	Ti(IV)	0	3.35	137.1	19.8
XISHUC	Ti(IV)	0	2.69	164.7	12.4
RIRLIN	Mo(IV)	+1	2.75	125.8	23.8
DOGHEM	Co(III)	+1	2.51	121.6	11.1
KERBUE	Co(III)	+2	2.91	111.2	14.1
KOLQUX	Co(III)	+1	2.70	120.5	13.9
MINJIC	Co(III)	+1	2.68	115.1	12.6
MINJOI	Co(III)	+1	2.62	118.1	12.2

<sup>a</sup> Definitions of the geometrical parameters are given in Figure 1.  
<sup>b</sup> References for crystal structures are given in Supporting Information.

mainly located on hydrogen atoms of acetylacetonato ring. On the other hand, the larger partial positive charge on the hydrogen atoms of phenyl ring favors the interaction, and the interaction is quite strong.

In the structures with intramolecular CH/ $\pi$  interactions with the chelate ring acting as a hydrogen atom acceptor (Table 3), one cannot expect to find correlation of the H- $\Omega$  distances with the geometry of the complex or with the type of metal in the chelate ring because, in the intramolecular interactions, steric constraints predetermine the geometry of the eventual interaction.

**Quantum Chemical Calculations.** Quantum chemical calculations were done on the model systems. The systems were made from the crystal structures of acetylacetonato complexes in the way that large groups in the complex were substituted by the hydrogen atoms. The energies were calculated for interactions of these model systems with benzene.

**Calculated Energies.** Calculated Energies for the MLCH/ $\pi$  Interactions. The model systems (Figure 6a) for calculations of the interactions of the CH group were made from the ACXMPD<sup>27</sup> crystal structure. Single-point calcula-

(24) Walther, D.; Stollenz, M.; Bottcher, L.; Gorls, H. Z. *Anorg. Allg. Chem.* **2001**, *627*, 1560–1570.

(25) Hasegawa, T.; Lau, T. C.; Taube, H.; Schaefer, W. P. *Inorg. Chem.* **1991**, *30*, 2921–2928.

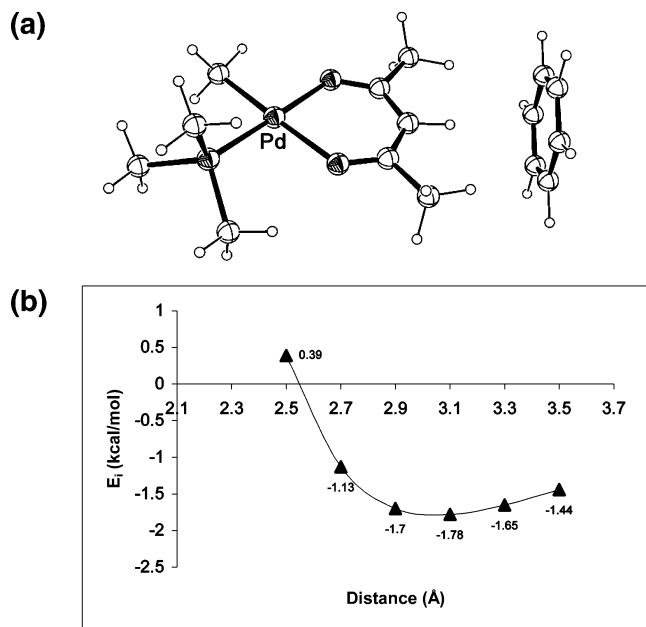


**Figure 6.** (a) ORTEP drawing of the model system for the calculations of the CH–phenyl interactions. (b) The curve shows the single-point MP2 energies for different H– $\Omega$  distances in the model system for CH–phenyl interactions.

tions were done for the H– $\Omega$  distances from 2.5 to 3.5 Å. The results of the calculations are shown in Figure 6b. For the distances below 2.6 Å, the interaction is repulsive. At a distance of 2.7 Å, the energy of the interactions is more than 1 kcal/mol. This is in agreement with experimental data where the interaction with the distance below 2.7 Å was not observed (Table 1 and Figure 2b).

The minimum is at 3.1 Å with an energy of interaction of 1.78 kcal/mol. There is quite a strong attractive interaction even at a distances of 3.5 Å: it is 1.44 kcal/mol.

The model system for calculating the interacting energy of the CH<sub>3</sub> group (Figure 7a) was made from the EHOVEC<sup>28</sup> crystal structure. Single-point calculations were done for H– $\Omega$  distances from 2.1 to 3.5 Å (Figure 7b). At a distance of 2.3 Å, the energy of the interactions is 0.97 kcal/mol. The most favorable interactions are 1.65 kcal/mol at distances of 2.6 and 2.7 Å. The interaction at 3.5 Å is 0.91 kcal/mol, smaller than that of the CH group (Figure 6b).

The energy minimum found between 2.6 and 2.7 Å is in agreement with the experimental data (Figure 3b). The large number of interactions observed at the distances above 3.0 Å is a consequence of the interactions of the phenyl ring not only with one but with two or three hydrogen atoms. In other words, for the long H– $\Omega$  distance, the phenyl ring can interact with another hydrogen atom of the methyl group making the overall interaction stronger.

The energy diagram of the interaction involving the CH group is quite different from diagram of the CH<sub>3</sub> group: the minimum is at a different distance, and the energy at the

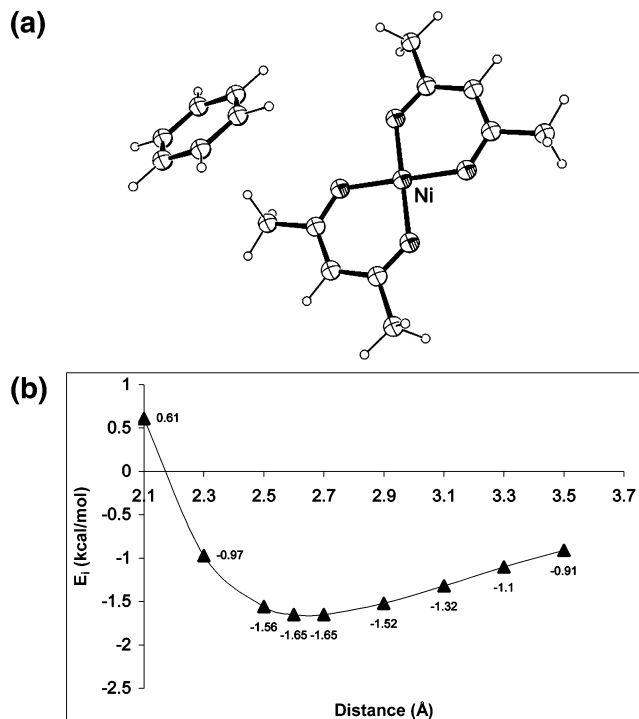


**Figure 7.** (a) ORTEP drawing of the model system for the calculations of the CH<sub>3</sub>–phenyl interactions. (b) The curve shows the single-point MP2 energies for different H– $\Omega$  distances in the model system for CH<sub>3</sub>–phenyl interactions.

minimum is different (Figure 6b and 7b). As was already mentioned for the experimental data of the CH group, longer distances are a consequence of steric clashing of the phenyl ring with the CH<sub>3</sub> groups.

The larger interacting energy for the longer H– $\Omega$  distances is consequence of the involvement of CH<sub>3</sub> groups in the interaction with the benzene ring. When the H– $\Omega$  distance is 3.1 Å, H atoms from the CH<sub>3</sub> groups are at the distance of 3.7 Å from the center of the benzene ring with  $\alpha$  and  $\beta$  angles of 152.9 and 38.3°, respectively. For these geometrical parameters, one can expect weak attractive interactions, and it makes the minimum energy for the CH group lower. To check this, we did calculations for interactions without methyl groups; we removed the CH<sub>3</sub> groups from our model system (Figure 6a) The calculated interacting energy at H– $\Omega$  distances of 3.1 Å is smaller: it is 1.06 kcal/mol. Hence, what we termed “interaction with the CH group” is not only an interaction with the CH group but also with the methyl groups.

**Calculated Energies for CH/ $\pi$  Interaction with the acac Chelate Ring as the Hydrogen Atom Acceptor.** The calculation of the interaction of the hydrogen atom of the phenyl ring with the  $\pi$ -system of the chelate ring was performed on the model system shown in Figure 8a. The model system was made from the XIBRUV<sup>24</sup> crystal structure. The calculated energies were shown in Figure 8b. At a distance of 2.3 Å, the energy of the interaction is 1.24 kcal/mol. The most favorable interaction is at H– $\Omega$  distances of 2.6 Å, and the energy is 1.62 kcal/mol. The minimum is almost at the same distance as the minimum for the CH/ $\pi$  interactions with the CH<sub>3</sub> group (Figure 7b), and the

(26) Suzuki, T.; Kashiwabara, K.; Kita, M.; Fujita, J.; Kaizaki, S. *Inorg. Chim. Acta*, **1998**, *281*, 77–84.

(27) Zenitani, Y.; Inoue, K.; Kai, Y.; Yasuoka, N.; Kasai, N. *Bull. Chem. Soc. Jpn.* **1976**, *49*, 1531–1537.

(28) Cui, Y.; Ngo, H. L.; Lin, W. *Chem. Commun.* **2003**, 1388–1389.

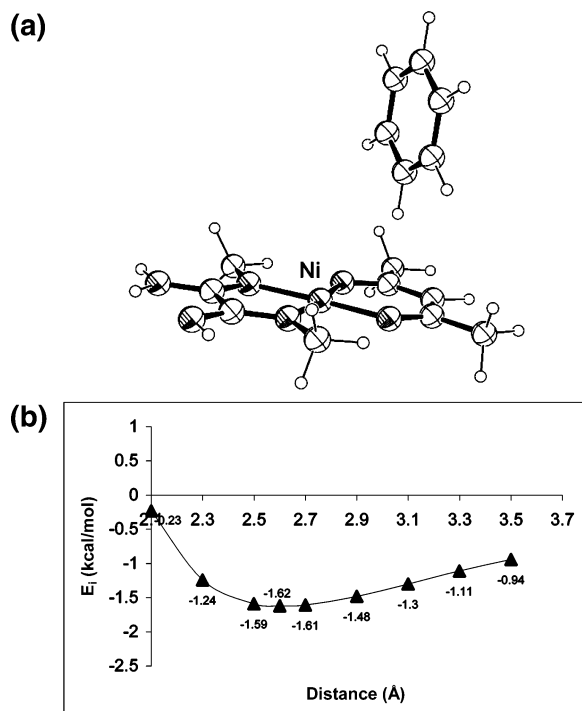


**Figure 8.** (a) ORTEP drawing of the model system for the calculations of the CH-chelate interactions. (b) The curve shows the single-point MP2 energies for different H- $\Omega$  distances in the model system for CH-chelate interactions.

interacting energies at the minimums are similar. The curves on the diagrams are very similar for these two types of interactions (Figures 7b and 8b), indicating that nature of these interactions could be similar.

**Metal-Dependent Capacity for CH/ $\pi$  Interactions.** As discussed above, the H- $\Omega$  distances in the crystal structures indicate the metal-dependent capacity for CH/ $\pi$  interactions of the acetylacetonato chelate. For the MLCH/ $\pi$  interactions, the H- $\Omega$  distances are shorter in complexes with soft metals (Figures 2b and 4). For the CH/ $\pi$  interactions with the  $\pi$ -system of the chelate ring in the square-planar complexes, it seems that the H- $\Omega$  distances are shorter with borderline metals than in the complexes with soft metals (Figure 5b).

To support these observations, we performed quantum chemical calculations of the partial charges and interacting energies. Since the trans effect and the charge of the complex can influence the interactions, the influence of a metal can be observed only if we compare complexes with the same structure and different metals. It was not possible to compare the hard metals with the soft metals because they do not make the same type of complexes. Soft metals make square-planar complexes, while hard metals make octahedral complexes (Table 2). The calculations were done on neutral complexes: [M(acac)<sub>2</sub>] complexes of borderline (Ni(II)) and soft acids (Pd(II), Pt(II)) (Figure 9) and [M(acac)(en)] complexes of soft acids (Rh(I) and Ir(I)).

The geometries of the [M(acac)<sub>2</sub>] and [M(acac)(en)] complexes were optimized, and NBO partial charges were calculated (Table 4). The positive partial charge on the metal decreases in [M(acac)<sub>2</sub>] in the order Ni, Pd, and Pt, and in [M(acac)(en)], it decreases from Rh to Ir. With the decrease

of the positive partial charge on metal, there is an increase of the positive partial charges on hydrogen atoms of acac (Table 4). It shows that if the metal is a softer acid, there is better delocalization of negative charge of acac ligand and more positive charge of the metal is transferred to the ligand.

The MP2 interacting energies between benzene and acac CH and CH<sub>3</sub> groups, corrected for BSSE, were calculated at the H- $\Omega$  distances of 3.1 and 2.6 Å, respectively, since we found out that the strongest interactions occur at those distances (Figures 6b and 7b). The calculated energies are given in Table 5. The increase in the interacting energies from Ni to Pt in the [M(acac)<sub>2</sub>] complexes and from Rh to Ir in the [M(acac)(en)] complexes for both the CH and CH<sub>3</sub> groups are in agreement with an increase of partial positive charge on the hydrogens of the acac ligand (Table 4) and with the experimental data (Figures 2b and 4). The results also show that oxidation state of the metal and other ligands in the complex have strong influence on interacting energies. The calculated interacting energies are larger for the [M(acac)<sub>2</sub>] complexes than for [M(acac)(en)] complexes (Table 5).

The interacting energies of the CH group of benzene with the  $\pi$ -system of the chelate ring were calculated for [M(acac)<sub>2</sub>] (M = Ni, Pd, Pt) and [M(acac)(en)] (M = Rh, Ir) complexes at a H- $\Omega$  distance of 2.6 Å because the strongest interaction is at that distance (Figure 8b). The calculated energies are in range from 1.58 to 2.62 kcal/mol (Table 5). The interacting energies of the [M(acac)<sub>2</sub>] complexes for borderline acid (Ni(II)) and soft acids (Pd(II) and Pt(II)) are very similar, while the energies for the [M(acac)(en)] complexes of the two soft acids (Rh(I) and Ir(I)) are quite different.

The data show that the interacting energies of benzene with the  $\pi$ -system of the acac chelate ring do not depend on the hardness of a metal or on the partial atomic charges, as was case for interactions where acac was the hydrogen atom donor. A comparison of the results for the [M(acac)<sub>2</sub>] complexes with those for the [M(acac)(en)] complexes show that the CH/ $\pi$  interactions where acac is a hydrogen atom donor are stronger for the [M(acac)<sub>2</sub>] complexes, while the CH/ $\pi$  interactions where acac acts as a hydrogen atom acceptor are stronger for the [M(acac)(en)] complexes (Table 5). This could suggest that the factors that favor interactions where acac is the hydrogen atom donor disfavor interactions where the acac chelate ring is the hydrogen atom acceptor. This is in agreement with observations that in the crystal structures of square-planar complexes, complexes with borderline acids make stronger CH/ $\pi$  interactions with  $\pi$  system of acac than complexes with soft acids (Figure 5b). However, that is not in agreement with the data for the [M(acac)(en)] complexes. Since the MLCH/ $\pi$  interactions are stronger for Ir(I) than for the Rh(I) complex (Table 5), one can anticipate that the CH/ $\pi$  interactions with the  $\pi$ -system of acac would be weaker for the Ir(I) complex. However, the data show the opposite: the Ir(I) complex makes stronger interactions (Table 5).

This suggests that the CH/ $\pi$  interactions where the  $\pi$ -system of the acac chelate ring is a hydrogen acceptor do not depend only on the delocalization of negative charge in



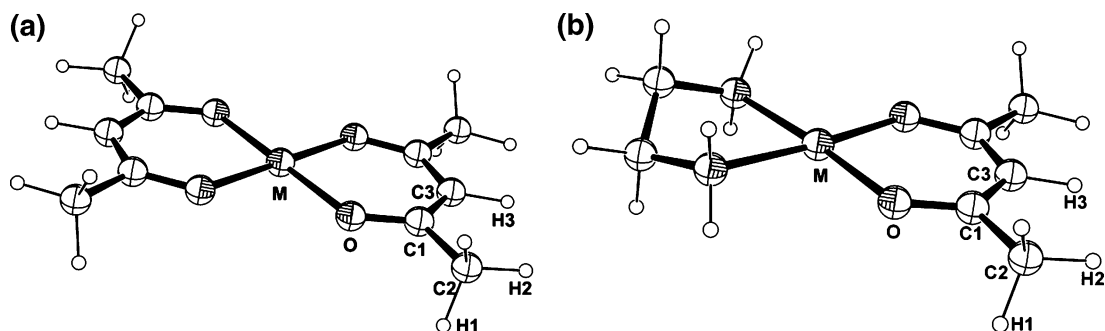


**Figure 9.** Model systems for calculating partial charges: (a)  $[M(\text{acac})_2]$  ( $M = \text{Ni}, \text{Pd}, \text{and Pt}$ ) and (b)  $[M(\text{acac})(\text{en})]$  ( $M = \text{Rh}$  and  $\text{Ir}$ ).

**Table 4.** Calculated Partial Atomic Charges<sup>a</sup> of  $[M(\text{acac})_2]$  ( $M = \text{Ni}, \text{Pd}, \text{Pt}$ ) and  $[M(\text{acac})(\text{en})]$  ( $M = \text{Rh}, \text{Ir}$ ) Complexes

atom	charge	atom	charge	atom	charge	atom	charge	atom	charge
Ni	1.4979	Pd	1.3175	Pt	1.2352	Rh	0.4848	Ir	0.3635
O	-0.8691	O	-0.8247	O	-0.8116	O	-0.8075	O	-0.7873
C1	0.6790	C1	0.6801	C1	0.6802	C1	0.6634	C1	0.6552
C2	-0.7136	C2	-0.7122	C2	-0.7118	C2	-0.7077	C2	-0.7060
C3	-0.6281	C3	-0.6352	C3	-0.6303	C3	-0.6392	C3	-0.6258
H1	0.2503	H1	0.2509	H1	0.2523	H1	0.2385	H1	0.2403
H2	0.2245	H2	0.2251	H2	0.2262	H2	0.2186	H2	0.2201
H3	0.2363	H3	0.2362	H3	0.2374	H3	0.2208	H3	0.2233

<sup>a</sup> Calculations were done using the natural bond orbital method from the MP2 wave function (see text for more details).

**Table 5.** Calculated Energies<sup>a</sup> of CH/ $\pi$  Interactions (kcal/mol) for  $[M(\text{acac})_2]$  ( $M = \text{Ni}, \text{Pd}, \text{Pt}$ ) and  $[M(\text{acac})(\text{en})]$  ( $M = \text{Rh}, \text{Ir}$ )

type of interactions	Ni	Pd	Pt	Rh	Ir
CH(acac)–benzene	2.12	2.26	2.34	1.44	1.51
CH <sub>3</sub> (acac)–benzene	1.64	1.76	1.89	0.64	0.73
CH(benzene)–chelate	1.60	1.58	1.59	2.42	2.62

<sup>a</sup> Calculations were done using the MP2//B3LYP method with LANL2DZ and 6-31G\*\* basis sets (see text for more details).

the acac chelate ring (and on hardness of a metal and on partial atomic charges) but on other factors too.

## Conclusions

In the acetylacetonato complexes, two types of CH/ $\pi$  interactions are possible: interactions of the hydrogen atoms of the ligand with the  $\pi$ -system of the phenyl ring (MLCH/ $\pi$  interactions) and interactions of the hydrogen atoms of the phenyl ring with the  $\pi$ -system of the metal–ligand chelate ring. A number of crystal structures with both types of interactions were found in CSD.

Most of the acetylacetonato complexes that have CH/ $\pi$  interactions with phenyl groups, in their crystal structures, are neutral complexes regardless of the type of interaction. Typically, the interaction occurs between two equivalent molecules of the complex: the phenyl group from one molecule interacts with the acetylacetonato chelate ring from another molecule. It indicates that, in neutral molecules, the partial charges on the phenyl and chelate rings are the driving forces for mutual interactions. In charged complexes, these local interactions are mainly overridden by ionic interactions.

Quantum chemical (MP2) calculations on a few model systems show that the energies of the CH/ $\pi$  interactions where the acetylacetonato ligand is the hydrogen atom donor (metal ligand CH/ $\pi$  (MLCH/ $\pi$ ) interactions) are in the range of 0.6–2.4 kcal/mol, while the energies of the CH/ $\pi$  interaction where the  $\pi$ -system of the acac chelate ring is the hydrogen atom acceptor are in the range of 1.5–2.7 kcal/mol.

The data suggest that electron delocalization mediates the metal-dependent capacity for the MLCH/ $\pi$  interactions. In the crystal structures, we observed shorter H– $\Omega$  distances for complexes with soft-acid metals. By quantum chemical calculations, it was shown that delocalization is better and energy of the interaction is larger in complexes with the soft metals. Consequently, better delocalization of the negative charge of the ligand (or transfer of positive charge from the metal) favors the MLCH/ $\pi$  interactions.

The data also suggest that CH/ $\pi$  interactions with the  $\pi$ -system of the acac chelate do not depend only on a hardness of a metal and on the delocalization of negative charge in the acac chelate ring but also on the other factors too.

**Acknowledgment.** The authors would like to thank Prof. E. W. Knapp and Prof. M. B. Hall for the support. This work was supported by the Serbian Ministry of Science (Grant 1795 and 142037).

**Supporting Information Available:** References for the crystal structures. This material is available free of charge via the Internet at <http://pubs.acs.org>.

IC051926G